

## Luminescence of BaBrI Crystals Doped with Ce<sup>3+</sup> Ions

R. Yu. Shendrik<sup>a,\*</sup>, I. I. Kovalev<sup>b</sup>, A. I. Rusakov<sup>a</sup>, Yu. V. Sokol'nikova<sup>a</sup>, and A. A. Shalaev<sup>a</sup>

<sup>a</sup> Vinogradov Institute of Geochemistry, Siberian Branch, Russian Academy of Sciences, Irkutsk, Russia

<sup>b</sup> Irkutsk State University, Irkutsk, Russia

\*e-mail: r.shendrik@gmail.com

Received December 4, 2018; accepted December 5, 2018

**Abstract**—The optical properties of BaBrI crystals doped with cerium ions are studied. The possible types of cerium-containing luminescence centres are established. Using the obtained experimental data for trivalent rare-earth elements, the Dorenbos diagram is constructed. The possible energy transfer mechanisms are proposed on the basis of results of studying the luminescence spectra measured with X-ray excitation.

DOI: 10.1134/S1063783419050329

### INTRODUCTION

At present, crystals of mixed alkaline earth metal halides doped with europium ions are promising scintillating materials [1]. The light yield of BaBrI–Eu crystals is estimated to be 90 000 photons/MeV [2] and the light yield of BaBrCl–Eu crystals is approximately 52 000 photons/MeV [3]. Despite the high light yield, a prolonged time of luminescence decay (about 400–500 ns) does not allow these crystals to be used in the registration systems, which require a high count rate. In these cases, crystals doped with cerium and praseodymium ions are basically used, since the time constant of luminescence decay of such materials does not exceed 40 ns [4].

In this study, we provide the data on studying the optical and scintillation properties of BaBrI crystals doped with cerium ions for the first time. Based on the analysis of the luminescence spectra for different types of excitation, the earlier described [5–7] energy level diagrams of rare-earth elements in the BaBrI crystal are clarified, and also conclusions on possible mechanisms of the energy transfer from the matrix to the cerium ions are drawn.

### EXPERIMENTAL

BaBrI crystals doped with CeBr<sub>3</sub> in different concentrations were grown by the Stockbarger method in vacuum sealed vials. The stoichiometric BaBr<sub>2</sub>–BaI<sub>2</sub>–CeBr<sub>3</sub> mixture was dried at temperatures of 80 and 300°C. The detailed batch preparation and crystal growth techniques are described in [5, 8]. Information on the content of the Ce ion impurity in BaBrI crystals was obtained by the method of mass spectrometry with inductively coupled plasma after dissolution of crystals and separating barium as the main component of the

matrix. An Element 2 high-resolution mass spectrometer (Finnigan MAT, Germany) was used for measurements. To construct the calibration curve, a series of solutions prepared from the standard CLMS-1 solution (Spex, United States) was used, in which the Ce concentration was in the range from 0.005 to 100 ng/mL. A solution of rhodium with a concentration of 2 ng/mL served as an internal standard. Significantly lower contents of Ce in comparison with the values calculated on the basis of the added amounts of additives were obtained in the analyses of samples. With a concentration of 0.5 mol % CeBr<sub>3</sub> in a batch, the cerium ion in a crystal was detected in a concentration of 10<sup>–3</sup> mol %. Perhaps, the CeOBr phase is formed upon drying the batch [9]. Hereinafter, the cerium ion concentrations obtained from the elemental analysis of crystals are given in this paper.

The luminescence and excitation spectra were measured on a Perkin-Elmer LS-55 spectrometer. The X-ray luminescence and low-temperature luminescence spectra were recorded on a system comprised of an MDR-2 monochromator and Hamamatsu 6780-04 photosensor module. Excitation was provided by an X-ray tube operating at 50 kV and 0.1 mA. The thermally stimulated luminescence curves were measured at a linear heating rate of 20 K/min.

The luminescence decay curves with photoexcitation by a pulsed nitrogen laser operating at a wavelength of 337 nm were measured by means of an MDR-2 monochromator, Hamamatsu 6780-04 photomultiplier module, and Rigol DS1202CA oscilloscope. X-ray excitation was provided by a MIRA-2D pulsed X-ray tube.

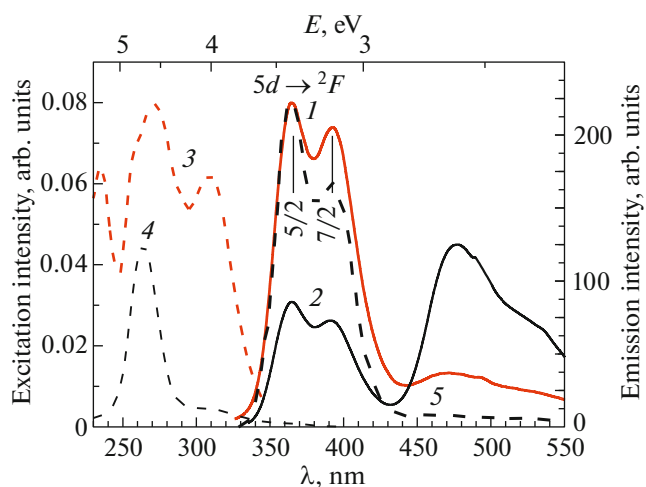


**Fig. 1.** Luminescence (solid curves) and excitation (dashed lines) spectra of BaBrI crystals doped with  $10^{-3}$  mol % (curves 1 and 3) and  $5 \times 10^{-4}$  mol % (curve 2)  $\text{CeBr}_3$ . The luminescence spectra (curves 1 and 2) were measured with excitation in the region of 310 nm; the excitation spectrum given in curve 3 was observed in the luminescence band at 370 nm and the excitation spectrum given in curve 4 was detected in the luminescence band at 500 nm. Curve 5 (dashed line) shows the luminescence spectrum with X-ray excitation.

## RESULTS AND DISCUSSION

Figure 1 shows the luminescence spectra of BaBrI crystals containing  $10^{-3}$  mol %  $\text{Ce}^{3+}$ , which were recorded with excitation in the region of 310 nm at room temperature. Two bands with the maxima at 364 and 392 nm or energies of 3.41 and 3.16 eV, as well as a broad band in the region of 480 nm are observed in the luminescence spectrum. Similar spectra were previously found in other crystals with similar structure, such as  $\text{BaBr}_2\text{-Ce}$  [10],  $\text{BaCl}_2\text{-Ce}$  [11], and  $\text{SrI}_2\text{-Ce}$  [12], and were associated with the luminescence of  $\text{Ce}^{3+}$  ions in different surrounding. Let us suppose that the luminescence with the doublet maxima at 364 and 392 nm is linked to site A. In that case, the luminescence in the region of 480 nm is associated with electronic transitions in site B. A two-fold decrease in the concentration of cerium ions in the crystal leads to an increase in the intensity of bands associated with luminescence centers is site B. At the same time, the intensity of the luminescence associated with site A decreases (Fig. 1, curve 2).

The excitation spectrum of site A is given in Fig. 1 (curve 3). The excitation spectra in both bands at 364 and 392 nm are equal: they contain several bands with maxima in the regions of 235, 260, 275, and 315 nm. In the excitation spectrum of site B, several bands with maxima at 260 and 310 nm can be also identified (Fig. 1, curve 4).

In the luminescence spectrum of site A, the distance between the doublet bands corresponds to spin-orbit splitting into the  ${}^2F_{7/2}$  and  ${}^2F_{5/2}$  terms (at approximately  $2000 \text{ cm}^{-1}$ ) in the  $\text{Ce}^{3+}$  ion. Thus, the observed luminescence is determined by the electronic transitions from the  $5d^1$  excited state to the  ${}^2F_{7/2}$  and  ${}^2F_{5/2}$  terms of the  $4f$  ground state split by spin-orbit coupling. The bands of site A in the spectrum of luminescence excitation are associated with the electronic transitions from the ground  $4f^1$  state to the  $5d$  state levels split by the crystal field.

The  $\text{Ce}^{3+}$  ion in BaBrI crystals substitutes the  $\text{Ba}^{2+}$  ion. Therefore, local compensation of the charge is required. This can be done either by interstitial  $\text{I}^-$  and  $\text{Br}^-$  ions or by  $\text{O}^{2-}$  oxygen impurity occupying a position in one of the crystal lattice sites of  $\text{I}^-$  or  $\text{Br}^-$  ions. By analogy with the previously obtained results [10, 11], we believe that the luminescence sites of type A are  $\text{Ce}^{3+}$  ions with the charge compensated by interstitial  $\text{I}^-$  or  $\text{Br}^-$  ions. A number of bands associated with the splitting of the  $5d$  state excited by the crystalline field is observed in the excitation spectrum. The smallest energy value for the  $4f\text{-}5d$  transition in the  $\text{Ce}^{3+}$  ion can be calculated from the excitation spectrum and it equals  $E_{fd} = 4 \text{ eV}$ . One can also estimate the centroid redshift ( $\epsilon_c$ ) and the Coulomb repulsion energy  $U(6, A)$  in the Dorenbos model [13, 14], which equal  $\epsilon_c = 2 \text{ eV}$  and  $U(6, A) = 6.57 \text{ eV}$ , respectively. These values are close to the values obtained in [5–7] for the  $\text{BaBrI-Eu}^{2+}$  system ( $U(6, A) = 6.4 \text{ eV}$  and  $E_{fd} = 4.2 \text{ eV}$ ).

The sites of the B type are cerium ions, the charges of which are compensated by oxygen ions. For the  $\text{BaF}_2\text{-Ce}$  crystal, this kind of site has been studied in detail in [15]. It has been shown that such sites represent the molecular centers, in which the ground state is mainly formed by  $4f^1$  levels of the  $\text{Ce}^{3+}$  ion and the excited is a superposition of the  $5d$  level of the  $\text{Ce}^{3+}$  ion and  $2p$  level of the oxygen ion. Since the transition to the ground state occurs from a large number of close levels, a broad band is observed in a luminescence spectrum. With X-ray excitation at room temperature, only the luminescence of sites A is observed (Fig. 1, curve 5). The light yield of the  $\text{BaBrI-}10^{-3}$  mol %  $\text{Ce}^{3+}$  crystal can be estimated comparing the integral X-ray luminescence intensities of the  $\text{BaBrI-Ce}$  and  $\text{CaF}_2\text{-Eu}^{2+}$  crystals with a known luminous yield of 19000 photons/MeV. The approximate value of the light yield in the  $\text{BaBrI-}10^{-3}$  mol %  $\text{Ce}^{3+}$  crystals is 15000 photons/MeV. It should be noted that the excitation band of sites A is almost completely overlapped by the luminescence band of excitons in BaBrI [5, 6] (Fig. 2); therefore, the resonance energy transfer from the excitons to sites A is possible by the Förster–Dexter mechanism [16].

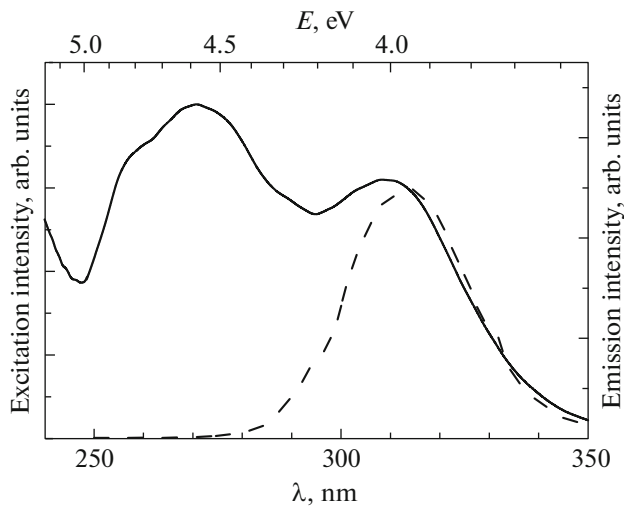


**Fig. 2.** Spectra of the  $4f-5d$  excitation of  $Ce^{3+}$  ions in sites A (solid curve) measured at room temperature, and the luminescence spectrum of autolocalized excitons at 77 K (dashed curve).

The luminescence decay curve measured in the band at 392 nm with photoexcitation is shown in Fig. 3a. Two components at 28 and 230 ns are observed in it. The spectra measured with temporal resolution revealed that the luminescence glow intensity with a decay constant of 230 ns is higher in the long-wave region at 475 nm. Thus, it can be concluded that the luminescence decay constant is linked to the sites B at 230 ns and to sites A at 28 ns. Two components in the luminescence decay are caused by superposition of two spectra.

With X-ray excitation, the shape of the curve of luminescence decay changes. The luminescence intensity decreases hyperbolically rather than exponentially (Fig. 3b). If this curve is represented as a sum of several exponential functions, the following components make the main contribution to the curve: the components corresponding to 30 and 520 ns, and 5  $\mu$ s. Their contributions to the total intensity are 57, 24, and 18%, respectively. The more prolonged components contribute less than one percent to the luminescence decay curve.

With photoexcitation of the crystal cooled to 80 K, the luminescence intensity practically does not depend on temperature, whereas the luminescence intensity with X-ray excitation significantly decreases upon a decrease in the temperature. A two-fold decrease in the intensity is observed upon cooling to 250 K (Fig. 4, curve 1). In the samples irradiated at 80 K, thermally stimulated luminescence (TSL) in the region of luminescence of sites A was observed upon heating. The TSL curve with a maximum at a temperature of 225 K is shown in Fig. 3 (curve 2).

The presence of nonexponential X-ray luminescence decay at room temperature and a decrease in its

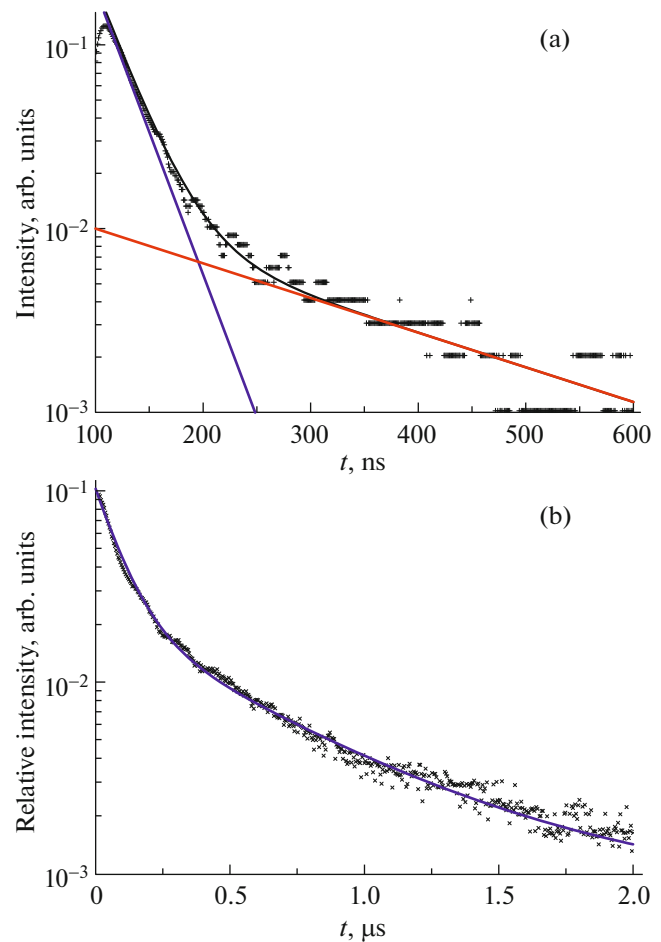


**Fig. 3.** Decay curves of the  $5d-4f$  luminescence of  $Ce^{3+}$  ions in the BaBrI crystal in the cases of (a) photoexcitation at 337 nm and (b) pulsed X-ray excitation.

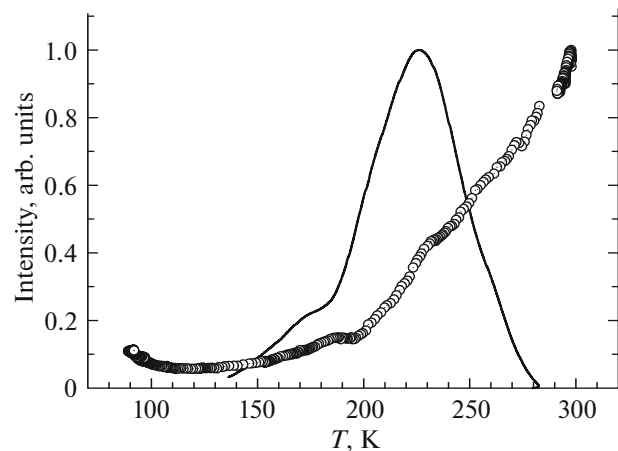


**Fig. 4.** Temperature dependence of the X-ray luminescence of sites A in BaBrI crystals with  $10^{-3}$  mol % of  $Ce^{3+}$  ions and TSL curve of the sample irradiated at 80 K measured in the band at 395 nm.

intensity in the region of TSL peak points to the participation of traps in the processes of energy transfer from the crystal lattice to the  $\text{Ce}^{3+}$  sites. Similar dependences have previously been studied in detail in the  $\text{CaF}_2$ ,  $\text{SrF}_2$ , and  $\text{BaF}_2$  crystals doped with  $\text{Pr}^{3+}$  ions [17, 18]. It was found that a rare-earth ion in these crystals is an electron trap and transforms from the trivalent state into the bivalent state after capturing an electron, while the hole is localized in the so-called “ $V_{\text{KA}}$ ” sites that are stable up to 250 K. Thermally stimulated motion of the holes starts at higher temperatures, which are recombined with electrons on the bivalent rare earth ions. As a result, the  $5d-4f$  luminescence of the trivalent rare earth ion is observed.

Thus, there are several possible mechanisms for the transfer of energy from the “hot” electrons and holes to the  $\text{Ce}^{3+}$  sites in the BaBrI–Ce crystals. First, the resonance energy transfer from excitons by the Förster–Dexter mechanism is possible, in which the excitons serve as donor centers and sites A serve as acceptors. Due to the substantial overlap of the excitation spectra of sites A and the luminescence spectra of excitons, the resonance mechanism must be effective. This allows one to expect an increase in the light yield in the BaBrI–Ce crystals with an increase in the dopant concentration.

Secondly, there is a “delayed” energy transfer process [18], in which hole sites are apparently involved, as shown earlier for the  $\text{BaBr}_2$ –Ce [11] and  $\text{SrI}_2$ –Ce [12] crystals. The presence of this process leads to the emergence of an additional component in the luminescence decay of cerium ions, which is associated with the recombination of an electron on the  $\text{Ce}^{2+}$  ion with holes distributed at various distances from the  $\text{Ce}^{2+}$  sites. Nevertheless, the contribution of the “delayed” energy transfer process is not so large even in crystals with a low concentration of cerium ions, since the X-ray luminescence decay curve predominantly contains the component corresponding to 30 ns. Therefore, one should expect a further decrease in the contribution of “delayed” energy transfer with an increase in the concentration of cerium ions. Based on the data given for alkaline earth fluorides doped with cerium [19], as well as for the BaBrI–Eu crystals [2], the optimal concentration of cerium ions must be in the range of 0.3–1 mol %  $\text{Ce}^{3+}$ .

## CONCLUSIONS

The results of studying the luminescence of the BaBrI–Ce crystals are given in this article. Two types of luminescence sites are formed in the BaBrI crystals after doping with cerium ions. In one case, the charge of the cerium ion is compensated by the interstitial iodine or bromine ion. The luminescence of such sites is observed not only with photoexcitation, but also with X-ray excitation. The second type of luminescence sites is associated with  $\text{Ce}^{3+}$  ions whose charge is

compensated by oxygen  $\text{O}^{2-}$  ions. With X-ray excitation at room temperature, no luminescence sites of this type are observed. With photoexcitation, these two types of sites differ by the luminescence decay time constant. This equals 28 ns for the first type of sites and 230 ns for the second type of sites.

On the basis of studying the TSL curves, the temperature dependence of the X-ray luminescence intensity, and the X-ray luminescence decay curves, possible mechanisms of energy transfer from the crystal lattice to the dopant ions in the BaBrI–Ce are assumed, namely: the resonant energy transfer from excitons and the “delayed” energy transfer mechanism involving hole sites. The studies carried out in this work allow one to conclude that the BaBrI–Ce crystals are promising for the use as fast scintillators.

## FUNDING

This work was supported by the Russian Science Foundation, grant no. 17-72-10084, in the part related to the spectroscopy of cerium and the cerium–oxygen sites, determination of the concentration of cerium in crystals, an analysis of the obtained results. Some of the studied crystals were grown within the State Assignment no. 0350-2016-0024.

## ACKNOWLEDGMENTS

The experimental data in this study were obtained using the scientific equipment of the Center for Collective Use Isotopic-Geochemical Studies of the Institute of Geochemistry, Siberian Branch, Russian Academy of Sciences.

## REFERENCES

1. G. Gundiah, G. Bizarri, S. M. Hanrahan, M. J. Weber, E. D. Bourret-Courchesne, and S. E. Derenzo, *Nucl. Instrum. Methods Phys. Res., Sect. A* **652**, 234 (2011).
2. E. Bourret-Courchesne, G. Bizarri, R. Borade, G. Gundiah, E. Samulon, Z. Yan, and S. Derenzo, *J. Cryst. Growth* **352**, 78 (2012).
3. Z. Yan, T. Shalapska, and E. Bourret, *J. Cryst. Growth* **435**, 42 (2016).
4. C. Dujardin, E. Auffray, E. Bourret-Courchesne, P. Dorrenbos, P. Lecoq, M. Nikl, A. N. Vasil'ev, A. Yoshikawa, and R.-Y. Ahu, *IEEE Trans. Nucl. Sci.* **65**, 1977 (2018).
5. R. Shendrik, A. Shalaev, A. Myasnikova, A. Bogdanov, E. Kaneva, A. Rusakov, and A. Vasilkovskiy, *J. Lumin.* **192**, 653 (2017).
6. A. Shalaev, R. Shendrik, A. Myasnikova, A. Bogdanov, A. Rusakov, and A. Vasilkovskiy, *Opt. Mater.* **79**, 84 (2018).
7. R. Shendrik, A. Myasnikova, A. Rupasov, and A. Shalaev, *Rad. Meas.* **122**, 17 (2019).
8. A. A. Shalaev, A. I. Rusakov, R. Yu. Shendrik, A. K. Subanakov, Yu. V. Sokol'nikova, and A. S. Myasnikova, *Phys. Solid State* **61**, 789 (2019).

9. A. Iltis, A. M. R. Mayhugh, P. Menge, C. M. Rozsa, O. Selles, and V. Solovyev, *Nucl. Instrum. Methods Phys. Res., Sect. A* **563**, 359 (2006).
10. G. Corradi, *J. Phys.: Condens. Matter* **16**, 1489 (2004).
11. J. Selling, G. Corradi, M. Secu, and S. Schweizer, *J. Phys.: Condens. Matter* **17**, 8069 (2005).
12. E. V. van Loefm, C. M. Wilson, N. J. Cherepy, G. Hull, S. A. Payne, W.-S. Choong, and W. W. Moses, *IEEE Trans. Nucl. Sci.* **56**, 869 (2009).
13. P. Dorenbos, *J. Lumin.* **136**, 122 (2013).
14. P. Dorenbos, *Phys. Rev. B* **85**, 165107 (2012).
15. R. Visser, P. Dorenbos, C. W. E. van Eijk, A. Meijerink, G. Blasse, and H. W. den Hartog, *J. Phys.: Condens. Matter* **5**, 1659 (1993).
16. B. Henderson and G. F. Imbusch, *Optical Spectroscopy of Inorganic Solids*, Vol. 44 of *Monographs on the Physics and Chemistry of Materials* (Oxford Univ. Press, Oxford, 2006).
17. R. Shendrik, E. Radzhabov, and V. Nagirnyi, *IOP Conf. Ser. Mater. Sci. Eng.* **15**, 012083 (2010).
18. R. Shendrik and E. Radzhabov, *IEEE Trans. Nucl. Sci.* **59**, 2089 (2012).
19. R. Shendrik and E. Radzhabov, *IEEE Trans. Nucl. Sci.* **61**, 406 (2014).

*Translated by O. Kadkin*